Efficiency and Safety of AAV-Mediated Gene Delivery of the Human ND4 Complex I Subunit in the Mouse Visual System

John Guy,[1] *Xiaoping Qi,*[2] *Rajeshwari D. Koilkonda,*[1] *Tania Arguello,*[1] *Tsung-Han Chou,*[1] *Marco Ruggeri,*[1] *Vittorio Porciatti,*[1] *Alfred S. Lewin,*[3] *and William W. Hauswirth*[2]

Purpose. To evaluate the efficiency and safety of AAV-mediated gene delivery of a normal human ND4 complex I subunit in the mouse visual system.

Methods. A nuclear encoded human ND4 subunit fused to the ATPc mitochondrial targeting sequence and FLAG epitope were packaged in AAV2 capsids that were injected into the right eyes of mice. AAV-GFP was injected into the left eyes. One month later, pattern electroretinography (PERG), rate of ATP synthesis, gene expression, and incorporation of the human ND4 subunit into the murine complex I were evaluated. Quantitative analysis of ND4FLAG-injected eyes was assessed compared with green fluorescent protein (GFP)-injected eyes.

Results. Rates of ATP synthesis and PERG amplitudes were similar in ND4FLAG- and GFP-inoculated eyes. PERG latency was shorter in eyes that received ND4FLAG. Immunoprecipitated murine complex I gave the expected 52-kDa band of processed human ND4FLAG. Confocal microscopy revealed perinuclear expression of FLAG colocalized with mitochondria-specific fluorescent dye. Transmission electron microscopy revealed FLAG immunogold within mitochondria. Compared with Thy1.2-positive retinal ganglion cells (RGCs), quantification was 38% for FLAG-positive RGCs and 65% for GFP-positive RGCs. Thy1.2 positive-RGC counts in AAV-ND4FLAG were similar to counts in control eyes injected with AAV-GFP.

Conclusions. Human ND4 was properly processed and imported into the mitochondria of RGCs and axons of mouse optic nerve after intravitreal injection. Although it had approximately two-thirds the efficiency of GFP, the expression of normal human ND4 in murine mitochondria did not induce the loss of RGCs, ATP synthesis, or PERG amplitude, suggesting that allotopic ND4 may be safe for the treatment of patients with Leber hereditary optic neuropathy. (*Invest Ophthalmol Vis Sci.* 2009;50:4205–4214) DOI:10.1167/iovs.08-3214

A G-to-A transition at nucleotide 11778 in mitochondrial DNA (mtDNA) in the gene specifying the NADH dehydrogenase subunit 4 (ND4) of complex I, which results in an arginine-to-histidine substitution at amino acid 340, is responsible for half of the cases of Leber hereditary optic neuropathy (LHON), a disease that causes blindness in young adults.[1–3] Moreover, patients with the G11778A mutation in mtDNA have the poorest prognosis for spontaneous visual improvement. There is no effective therapy for LHON or, for that matter, for any other disease caused by mutated mtDNA. Unlike the other mitochondrial diseases in which the ratio of mutated to normal mtDNA determines phenotype (a condition called *heteroplasmy*), visual loss from LHON usually requires 100% mutated mtDNA (*homoplasmy*). Therefore, it is highly likely that the introduction of normal mtDNA into patients with LHON may protect against visual loss and blindness.

Any proposed therapy for LHON or other diseases caused by mutated mtDNA must wrestle with several problems: There is no way yet to correct mutated mtDNA in living animals; there is no delivery system for DNA into mitochondria; there is no confirmed evidence for recombination between mtDNA molecules that would enable gene replacement; and there are no selectable markers for mitochondrial transformation. We and others[4,5] have taken an alternative approach for correcting point mutations in mitochondrial protein-coding genes by expressing these genes in the nucleus in conjunction with an N-terminal targeting sequence for mitochondrial import. Most mitochondrial proteins are, in fact, made this way and are transported into the organelles after their translation on cytoplasmic polyribosomes. There are at least two major obstacles to correcting mitochondrial mutations in this way. First, mitochondrial translation makes use of a genetic code partially different from that of the nuclear-cytoplasmic system. Second, some mitochondrial proteins may be too hydrophobic to be imported and properly assembled from the "outside." The first obstacle can be addressed by completely recoding mitochondrial genes so that they can be expressed on cytoplasmic ribosomes,[6,7] an approach coined *allotopic expression*. This process involves using overlapping oligonucleotides to rebuild the genes in the universal genetic code, choosing codons that permit high-level translation,[8] or using in situ mutagenesis to change codons that differ between the mitochondria and the nucleus.[9]

The second problem is more difficult. Claros et al.[10] attempted import of a universal code version of apocytochrome *b* from the nucleus of yeast and found that each of the eight transmembrane helices of this protein could be transported separately into mitochondria but that no more than three or four of the hydrophobic domains could be transported as one peptide. They[10] and others[11,12] argue that the hydrophobicity of mitochondrial proteins imposes a limit on which genes could be transplaced to the nucleus, that allotopically expressed proteins do not integrate into host respiratory complexes, and that allotopically expressed proteins result in significant cytotoxicity, even inducing cell death. Rather than

From the [1]Bascom Palmer Eye Institute, University of Miami, Miller School of Medicine, Miami, Florida; and the Departments of [2]Ophthalmology and [3]Molecular Genetics and Microbiology, University of Florida, College of Medicine, Gainesville, Florida.

Supported by National Institutes of Health Grants R01EY017141 (JG), R24EY018600 (JG), and EY014801 (core center grant) and in part by Research to Prevent Blindness (Department of Ophthalmology).

Submitted for publication November 25, 2008; revised March 18, 2009; accepted June 17, 2009.

Disclosure: **J. Guy**, None; **X. Qi**, P; **R.D. Koilkonda**, None; **T. Arguello**, None; **T.-H. Chou**, None; **M. Ruggeri**, None; **V. Porciatti**, None; **A.S. Lewin**, P; **W.W. Hauswirth**, P

The publication costs of this article were defrayed in part by page charge payment. This article must therefore be marked "*advertisement*" in accordance with 18 U.S.C. §1734 solely to indicate this fact.

Corresponding author: John Guy, Bascom Palmer Eye Institute, 1638 NW 10th Avenue, Miami, FL 33136; jguy@med.miami.edu.

continue this debate in cultured cells, here we evaluated the potential value or pitfalls of allotopic expression of a normal human *ND4* gene in the mouse visual system, in which we previously demonstrated that allotopic expression of the mutant human R340H ND4 induced optic disc edema with the demise of retinal ganglion cells (RGCs) and axons of the optic nerve.[13]

METHODS

Construction of Human ND4FLAG and AAV Vectors

To construct the fusion gene containing the mitochondrial targeting sequences and epitope tag, synthetic 80-mer oligonucleotide pairs were created in the nuclear genetic code and codons prevalent in highly expressed nuclear genes to conserve amino acid sequence. The synthetic oligonucleotides were overlapped by approximately 20 complementary nucleotides serving as primers for PCR with the high fidelity of polymerase (*pfu* Turbo DNA; Stratagene, La Jolla, CA) until the entire 1377-nucleotide nuclear-encoded *ND4* gene was constructed. With this technique, the ND4 gene was then fused in-frame to the ATP1 and FLAG epitope tags. To complete generating the wild-type ND4, base deletions and substitutions in the reading frame were corrected with an in vitro mutagenesis kit (QuickChange; Stratagene). Flanking *Xba*I restriction sites were added for cloning the human P1ND4FLAG into AAV vectors. The entire reading frame of the human P1ND4FLAG fusion gene was cloned into the *Xba*I sites of AAV plasmid vector pTR-UF22, regulated by the 381-bp cytomegalovirus immediate early gene enhancer/1352-bp chicken β-actin promoter-exon1-intron1 woodchuck posttranscriptional regulatory element. Plasmids were amplified and purified by cesium chloride gradient centrifugation and then packaged into AAV-2 capsids by transfection into human 293 cells using standard procedures.[14] Genome titers of the recombinant AAV (rAAV) were determined using real-time PCR.[14] The resultant rAAV-packaged ND4 and humanized green fluorescent protein (GFP) control viruses were assayed, and each virus preparation contained 10^{11} to 10^{12} particles per milliliter.

Experimental Animals

All animal procedures were performed in accordance with the National Institutes of Health Guide for Care and Use of Laboratory Animals and the ARVO Statement for the Use Animals in Ophthalmic and Vision Research. For the intraocular injection of recombinant rAAV, 70 DBA/1J mice were sedated by inhalation with 1.5% to 2% isoflurane. A local anesthetic (proparacaine HCl) was applied topically to the cornea, and then a 32-gauge needle attached to a Hamilton syringe was inserted through the pars plana. Right eyes were injected with 2 μL AAV-ND4FLAG, and left eyes were injected with 2 μL control AAV vector containing the gene for GFP.

OCT Imaging

In vivo high-resolution three-dimensional (3D) imaging of the living mouse retina was performed with spectral-domain optical coherence tomography (OCT), as previously described.[15] Briefly, ketamine/xylazine-anesthetized mice ($n = 7$) were restrained in a mounting tube that was fixed on a six-axis platform. Raster scans—typically measuring 512 × 128 (horizontal × vertical) and 1024 × 64 depth scan patterns, with the fast scan in the horizontal direction—were performed for each eye. Scan length was approximately 32° for imaging mouse retinas. Acquisition of high-quality OCT images took approximately 5 minutes for each mouse eye.

PERG Recording

Pattern electroretinography (PERG) was measured in six mice, as previously reported.[16] In brief, ketamine/xylazine-anesthetized mice were gently restrained with the use of a bite bar and a nose holder that allowed unobstructed vision and were kept at a constant body temperature of 37°C with a feedback-controlled heating pad. In anesthetized mice, eyes were typically wide open and steady, with undilated pupils pointing laterally and upward. The ERG electrode (0.25-mm diameter silver wire configured to a semicircular loop of 2-mm radius) was placed on the corneal surface by means of a micromanipulator and was positioned in such a way as to encircle the pupil without limiting the field of view. Reference and ground electrodes were stainless steel needles inserted under the skin of the scalp and tail, respectively. A small drop of balanced saline topically applied on the cornea prevented drying for the duration of recording. A visual stimulus of contrast-reversing bars (field area, 50° × 58°; mean luminance, 50 cd/m^2; spatial frequency, 0.05 cyc/deg; contrast, 98%; temporal frequency, 1 Hz) was aligned with the projection of the pupil at a distance of 20 cm. Eyes were not refracted for the viewing distance given that the mouse eye has a large depth of focus because of the pinhole pupil. Retinal signals were amplified (10,000-fold) and bandpass filtered (1–30 Hz). Three consecutive responses to each of 600 contrast reversals were recorded. The responses were superimposed to check for consistency and then averaged. The PERG is a light-adapted response. To have a corresponding index of outer retinal function, a light-adapted ERG (FERG) was also recorded with undilated pupils in response to strobe flashes of 20 cd/m^2/s superimposed on a steady background light of 12 cd/m^2 and presented within a Ganzfeld bowl. Under these conditions, rod activity is largely suppressed, whereas cone activity is minimally suppressed. Averaged PERG and FERGs were automatically analyzed to evaluate the major positive and negative waves. Statistical analysis was performed by Student's *t*-test for unpaired data. $P < 0.05$ was considered statistically significant.

Oxidative Phosphorylation Assay

Optic nerves were dissected from seven mice. Tissues were homogenized and resuspended in buffer (150 mM KCl, 25 mM EDTA, 0.1% bovine serum albumin, 10 mM potassium phosphate, 0.1 mM $MgCl_2$, pH 7.4). The rate of ATP synthesis of excised tissues was measured by chemiluminescence using a modified luciferin-luciferase assay in digitonin-permeabilized tissues with the complex I substrates malate and pyruvate in real-time using a luminometer (Optocom I; MGM Instruments, Hamden, CT) and expressed per milligram of protein.

Flatmount Retina Preparation

One month after ocular viral injection, 40 mice were euthanatized, each with a lethal dose (100 mg/kg intraperitoneally) of pentobarbital sodium (Euthasol, 390 mg/mL; Virbac Animal Health, Inc., Fort Worth, TX). Then they underwent intracardial perfusion with phosphate-buffered saline (PBS) until blood was removed from the system, followed by the administration of 25 mL of 4% paraformaldehyde (pH 7.4). The eyes were quickly enucleated, and the cornea was punctured to allow fixative to penetrate the eye. Ten eyes with the corneas removed were incubated for 30 minutes at 37°C with 250 nM mitochondria-specific fluorescent dye (MitoTracker Green; Invitrogen-Molecular Probes, Carlsbad, CA). The other 30 eyes were subsequently postfixed in 4% paraformaldehyde (pH 7.4) for 30 minutes at 4°C before they were transferred to PBS for dissection. Anterior segments were carefully removed, and posterior eyecups containing retinas were then immersed in 4% paraformaldehyde in 0.1 M phosphate buffer, pH 7.4, for 30 minutes at 4°C. Whole retinas were gently separated from the eyecups, and they were flatmounted in a Maltese cross configuration on fine filter paper (no. 50; Whatman, Maidstone, Kent, UK). Each retina was rinsed extensively with PBS (pH 7.4) and transferred to a block medium consisting of 1% BSA and 1% normal goat sera in PBS (pH 7.4) with 0.1% Triton X-100 for immunostaining.

Immunohistochemistry

The flatmounted retinas were incubated with a mixture of mouse monoclonal anti–FLAG M2 antibodies conjugated to Cy3 (Sigma-Aldrich, St. Louis, MO) or rabbit anti–GFP antibodies (BD-Clontech, Palo

Alto, CA) for 24 hours at 4°C. Secondary goat anti–rabbit Cy2 (Jackson ImmunoResearch Laboratories, West Grove, PA) was used to detect rabbit anti–GFP on specimens. Immunofluorescence was visualized under a fluorescence microscope (Leitz, Wetzlar, Germany). Red or green filters were used to visualize FLAG-labeled mitochondria or GFP-labeled cells, respectively. To detect the RGCs we used monoclonal anti–Thy1.2 antibody (Abcam, Inc., Cambridge, MA) followed by secondary antibody conjugated with Cy3. Immunogold transmission electron microscopy was used for detection of the FLAG epitope. Subsequently, the resin (LR White; Electron Microscopy Sciences, Hatfield, PA) sections were rinsed in 0.01 M PBS (pH 7.4) and were incubated for 24 hours at 4°C with a mixture of primary mouse monoclonal anti–FLAG M2 antibodies and secondary goat anti–mouse IgG conjugated to 6 nm colloidal gold. For identification of mitochondria in resin (LR White; Electron Microscopy Sciences) sections, we costained with rabbit MnSOD antibody using secondary goat anti–rabbit IgG conjugated to 10 nm colloidal gold. Sections were then examined under transmission electron microscopy (H7600; Hitachi, Tokyo, Japan).

Quantitative Analysis

Flatmounted retinas were prepared and laid out with the RGC layer facing upward. In retinal wholemounts, the populations of ND4FLAG (10 mice), GFP (10 mice), and Thy1.2 + immunopositive RGC counts were performed by a masked observer who counted cells from the central optic disc toward the peripheral retinal regions, covering an area of 0.25 mm^2. The images were captured with a video camera mounted on a fluorescence microscope at magnification of 400×. We used ImageJ software (developed by Wayne Rasband, National Institutes of Health, Bethesda, MD; available at http://rsb.info.nih.gov/nih-image). Statistical analysis was performed by Student's *t*-test for unpaired data. $P < 0.05$ was considered statistically significant.

mRNA Analysis

Total RNA was isolated from 10 mouse optic nerves and retinas (RNeasy Protect Mini Kit; Qiagen, Valencia, CA). Reverse transcription PCR was performed with an RT-PCR system (Access; Promega, Madison, WI), human ND4-primer 5′-CGCTGTGATCCTGATGATCGCTCAC-3′, and antisense primer 5′- GTGATGTTGCTCCAGCTGAATGTTG-3′ with an expected PCR product size of 242 bp. Mouse β-actin sense primer was 5′-TCAGCAAGCAGGAGTACGATGA-3′, and the antisense primer was 5′- TGCGCAAGTTAGGTTTTGTCAA-3′ with a PCR product size of 117 bp. Resultant PCR products were electrophoresed on a 3% agarose gel and stained with ethidium bromide. After the bands were dissected from the gel, the target DNA in each band was eluted and sequenced.

Immunoprecipitation and Immunoblotting

Mitochondrial proteins were isolated from optic nerves and retinas of 20 mice infected with AAV-expressing human ND4, mouse heart tissue, or AAV-GFP–infected eyes as controls. Briefly, this involved washing tissues in cold PBS, followed by resuspension in a buffer consisting of 50 mM Tris-HCl, 0.21 M D-mannitol, 70 mM sucrose, 0.1 M phenylmethylsulfonyl fluoride, 3 mM $CaCl_2$, and 20 mM EDTA (pH 7.5). Tissues were then manually homogenized. The homogenates were centrifuged at 1200*g* for 10 minutes at 4°C. The resultant supernatant containing the mitochondrial fraction was collected and then centrifuged at 12,000*g* for 20 minutes at 4°C. The pellet containing the mitochondria was washed and resuspended in buffer consisting of 50 mM Tris-HCl, 10 mM EDTA, and 20% sucrose (pH 7.5), then stored at −80°C for later analysis.

We used a kit (MS101 Complex I Immunocapture Kit; Mito-Sciences, Eugene, OR) for the immunoprecipitation of complex I according to the manufacturer's specifications. Briefly, this involved resuspending the mitochondrial isolates in buffer that consisted of 50 mM Tris-HCl (pH 7.5), 1:100 protease inhibitor cocktail (Calbiochem EMD Biosciences, San Diego, CA), and 1 mM phenylmethylsulfonyl fluoride and then adding 100 μL of 10% N-dodecyl-β-D-maltoside. This mixture was incubated on ice for 30 minutes and then centrifuged for 30 minutes at 21,000*g* at 4°C. The beads saturated with antibody provided with the kit were then added. The suspension was incubated overnight at 4°C with gentle agitation. After a spin at 3200*g* for 3 minutes at 4°C, the pellet was washed with PBS plus 1% N-dodecyl-β-D-maltoside. To elute proteins, beads with bound complex I were resuspended in 40 μL of 1% SDS and incubated for 10 minutes at room temperature. After centrifugation at 3200*g* for 3 minutes at 4°C, the supernatant was saved and stored at −80°C for later analysis.

For Western blot analysis, proteins immunoprecipitated from mitochondria isolated from the optic nerves (5 μg) or retinas (7 μg) of rAAV-inoculated eyes were separated by electrophoresis through a 10% polyacrylamide gel and electrotransferred to a polyvinylidene fluoride membrane (Bio-Rad, Hercules, CA). For immunodetection, the membrane was stained with murine anti–FLAG M2 antibody (Sigma-Aldrich) and then with rabbit anti–mouse IgG horseradish peroxidase (HRP)-conjugated secondary antibodies (Sigma-Aldrich). We detected complexes using the enhanced chemiluminescence (ECL) system (GE Healthcare, Piscataway, NJ).

Results

mRNA Analysis

Agarose gel electrophoresis of the RT-PCR product obtained from the RNA extracted from the retina and optic nerve of eyes injected with AAV-P1ND4FLAG revealed the expected 242-bp band, indicating in vivo transcription of the nuclear encoded human ND4 (Fig. 1A, top, lanes 4 and 5). This band was absent in control eyes injected with AAV-GFP (Fig. 1A, top, lanes 2 and 3). Primers specific to the housekeeping β-actin mRNA showed the 117-bp band in all ocular tissues (Fig. 1A, bottom, lanes 2–5) but not with plasmid ND4FLAG serving as the template (Fig. 1A, bottom, lane 1). Sequencing of the PCR products (ND4) obtained from the retina and optic nerve confirmed that the amplified DNA was indeed the nuclear encoded human ND4 subunit of complex I.

Immunoprecipitation

Our next steps were to determine whether the human ND4FLAG fusion protein was expressed and imported into the mitochondria and whether it would incorporate into the murine holocomplex I. Mitochondrial fractions were prepared from retinas, and optic nerves were dissected from rAAV-injected mice. After immunoprecipitation of the murine complex I, immunoblots of the transferred proteins that were immunoreacted with the anti–FLAG M2 antibody revealed specific bands at 52 kDa for the retina and the optic nerve of eyes that received intravitreal injection of AAV containing the human nuclear encoded P1ND4FLAG (Fig. 1B, lanes 3 and 4). The higher molecular weight of uncleaved P1ND4FLAG was not evident.[13] Immunoprecipitation of the retina and optic nerve of control eyes inoculated with AAV-GFP or cardiac tissue (not shown) was negative for the ND4FLAG fusion protein (Fig. 1B, lanes 1 and 2). Thus, the nuclear encoded human ND4 complex I subunit was imported into the mitochondria, then it was processed by cleavage of the ATPc targeting sequence from the mature human ND4 fusion protein that was then incorporated into the murine complex I.

Efficiency of Allotopic Expression

Next, we sought to determine the efficiency of human ND4FLAG expression in the mouse retina compared with that of a commonly used marker of gene expression, the GFP. Low-power magnification of retinal flatmounts from eyes injected with AAV-P1ND4FLAG revealed a perinuclear pattern of

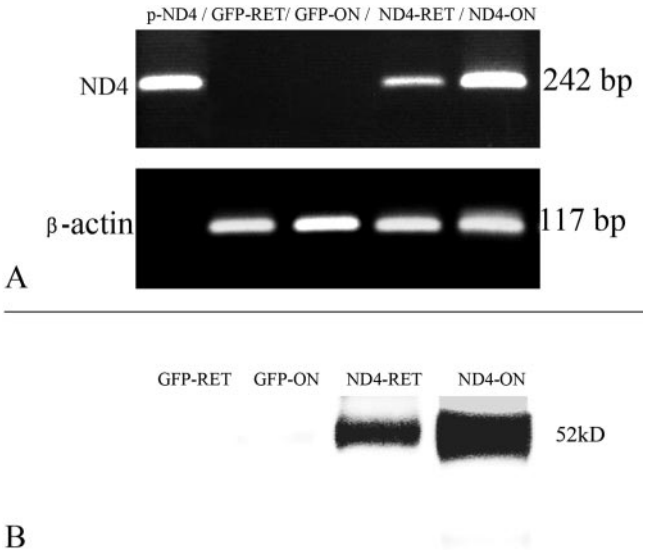

FIGURE 1. (**A**) Agarose gel electrophoresis of a positive control AAV-pTR plasmid containing the nuclear encoded ND4 shows the expected 242-bp band (*top, lane 1*). This band was absent in the retina (*top, lane 2*) and optic nerve (*top, lane 3*) of control eyes that were injected with AAV-GFP. In contrast, the RT-PCR product obtained from the RNA extracted from the retina and optic nerves of eyes injected with AAV-P1ND4FLAG revealed the expected 242-bp band, indicating in vivo transcription of the nuclear encoded human ND4 (*top, lanes 4, 5*). The housekeeping β-actin PCR product was seen in all ocular tissues (*bottom, lanes 2–5*), but it was absent with plasmid ND4FLAG serving as the template (*bottom, lane 1*). (**B**) Western blot analysis of immunoprecipitated murine complex I reacted with anti–FLAG M2 antibody revealed specific bands at 52 kDa for both the retina and the optic nerve of eyes that received intravitreal injection of AAV containing the human nuclear encoded *ND4FLAG* gene (**B**, *lanes 3, 4*). Western blot analysis of immunoprecipitated murine complex I extracted from the retina and optic nerve of control eyes inoculated with AAV-GFP were negative for the ND4FLAG fusion protein (**B**, *lanes 1, 2*). These findings suggest that the nuclear encoded human ND4 complex I subunit was incorporated into the mouse complex I. p-ND4, AAV plasmid containing the human *ND4* gene; GFP-RET, GFP-inoculated retina; GFP-ON, GFP-inoculated optic nerve; ND4-RET, ND4-inoculated retina; ND4-ON, ND4-inoculated optic nerve.

ND4FLAG immunofluorescence (Fig. 2A). In contrast, the pattern of GFP immunofluorescence in retinal flatmounts from control eyes revealed the typical cytoplasmic and nuclear patterns of localization in RGCs and along their axonal bundles of the nerve fiber layer (Fig. 2B). Nuclear staining with DAPI is shown in Fig 2C. Confocal microscopy clearly revealed the punctate and perinuclear pattern of ND4FLAG localization surrounding the nuclei of RGCs counterstained with DAPI (Fig. 2D). Identification of mitochondria was performed with mitochondria-specific fluorescent dye (MitoTracker Green; Invitrogen-Molecular Probes) that surrounded RGC nuclei counterstained with DAPI (Fig. 2E). Merging panel 2D with 2E showed that the ND4FLAG colocalized with the bona fide mitochondrial marker (Fig. 2F). Thus, the human ND4 was imported into murine mitochondria. Accumulation of the mitochondria-specific fluorescent dye (MitoTracker Green; Invitrogen-Molecular Probes) also indicated no loss of mitochondrial membrane potential in ND4-expressing cells. Longitudinal cryostat sections, counterstained with DAPI, revealed that ND4FLAG immunofluorescence was confined to the ganglion cell layer (Figs. 2G, 2J). Accumulation of mitochondria-specific fluorescent dye (MitoTracker Green; Invitrogen-Molecular Probes) in RGCs indicated that ND4FLAG expression did not cause loss of membrane potential (Figs. 2H, 2K). Colocalization of ND4FLAG and mitochondria-specific fluorescent dye (MitoTracker Green; Invitrogen-Molecular Probes) confirmed import of the allotopically expressed protein into the mitochondria (Figs. 2I, 2L).

To obtain the efficiency of allotopic expression in the mouse retina, we counted cells that expressed ND4FLAG compared with the total population of ganglion cells in the retina. RGCs were identified by Thy1.2 immunoreactivity. Compared with a mean value of 3176 ± 269 Thy1.2-positive RGCs/mm^2, ND4FLAG-positive RGCs had a mean value of 1226 ± 173 cells/mm^2 (Fig. 2M).

Thus, ND4FLAG was expressed in 38% of the RGCs. GFP expression was greater, labeling 65% of the RGCs. Compared with a mean of 3176 ± 269 Thy1.2-positive RGCs/mm^2, GFP-positive RGCs had a mean value of 2075 ± 309 cells/mm^2. Thus, the efficiency of allotopic ND4FLAG expression in vivo was two-thirds that of GFP ($P = 0.01$).

Safety of Allotopic ND4 Expression

OCT of Live Mice. Magnified cross-sectional montaged images of the optic nerve head and peripapillary retina from the acquired 3D OCT data set of an AAV-ND4 inoculated mouse eye (Fig. 3A) and the opposite eye of this mouse injected with AAV-GFP revealed normal retinal structures (Fig. 3B). The OCT image is displayed in grayscale, with darker readings corresponding to lower backscattering and brighter regions representing higher backscattering. The ganglion cell layers of experimental and control eyes were clearly recognizable. The optic nerve head of AAV-ND4 and control eyes showed no evidence of displacement of the peripapillary retina to suggest disc edema. We measured the distance from the RGC layer to the inner boundary of the inner nuclear layer for each acquired image. Using algorithms for 3D segmentation of this region of the retina provided a geometric plot in three dimensions for the AAV-ND4 (Fig. 3C) and AAV-GFP control eyes (Fig. 3D).

Light Microscopy. To determine whether human ND4 was toxic to ganglion cells of the murine retina, we evaluated the number of RGCs, identified by Thy1.2 immunoreactivity, in retinal flatmounts (Figs. 4A, 4B) of AAV-ND4FLAG–infected eyes compared with control eyes injected with AAV-GFP. Representative flatmounts of Thy1.2 positive-RGCs of AAV-ND4FLAG (Fig. 4C) and AAV-GFP (Fig. 4D) inoculated eyes appeared comparable, showing numerous RGCs. Toluidine blue sections of AAV-ND4FLAG–inoculated eyes (Fig. 4E) or AAV-GFP–inoculated eyes (Fig. 4F) showed no evidence of swelling of the optic nerve head, a common finding at this juncture in eyes inoculated with a mutant human R340H ND4.[13] Ganglion cells of the AAV-ND4FLAG–infected retina appeared normal (Fig. 4G). They showed no chromatolysis or loss and appeared comparable to those of AAV-GFP–injected eyes (Fig. 4H). These observations were confirmed next by quantitative analysis. With a mean value of 3176 ± 269 RGCs/mm^2 in AAV-ND4–injected eyes compared with a mean of 3316 ± 309 RGCs/mm^2 in control eyes injected with AAV-GFP, we detected no significant differences in RGC counts between experimental and control eyes ($P = 0.79$; Fig. 4I). Thus, AAV-mediated gene delivery of the human ND4 to the mouse retina does not appear detrimental to ganglion cell survival.

Ultrastructure. Next, potential mitochondrial abnormalities induced by expression of human ND4FLAG in murine mitochondria were investigated by transmission electron microscopy. For comparison, a representative micrograph of the optic nerve obtained from an animal that received no intraocular injection exhibiting normal mitochondrial ultrastructure is shown (Fig. 5A). Compared with the normal nerve, axonal mitochondria of an AAV-ND4FLAG–inoculated eye showed no evidence of swelling or disruption of cristae (Fig. 5B). RGC bodies with large, round, pale nuclear chromatin exhibited no condensation of the nucleus or cytoplasm to suggest apoptosis.

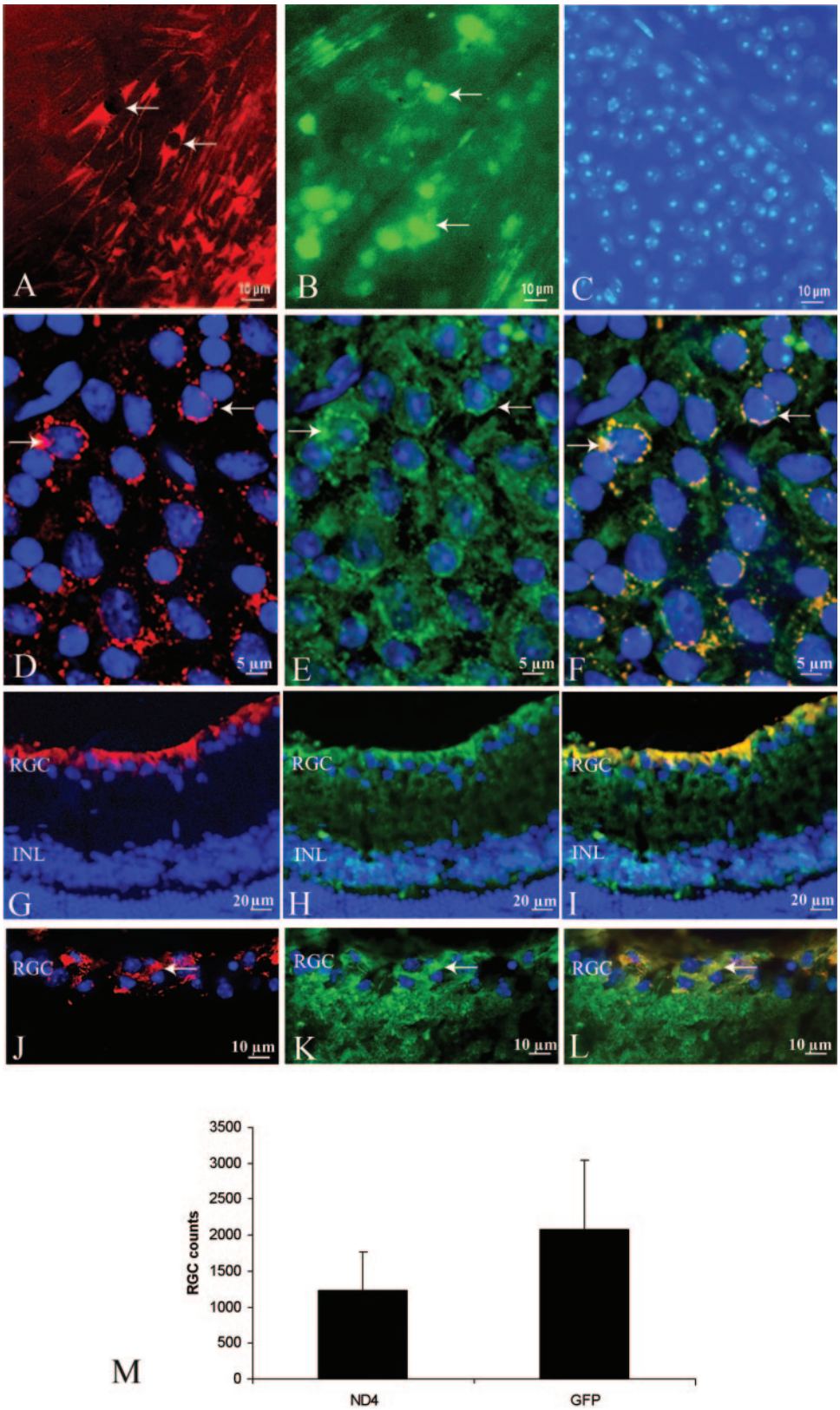

FIGURE 2. (**A**) Retinal flatmount from an eye injected with AAV-ND4FLAG revealed a perinuclear pattern of ND4FLAG immunofluorescence (*arrows*). (**B**) Retinal flatmount of a control eye injected with AAV-GFP showed a cytoplasmic and nuclear pattern of GFP immunofluorescence in RGCs (*arrows*) and along their axonal bundles of the nerve fiber layer. (**C**) Flatmount counterstained with DAPI shows the RGC nuclei. (**D**) Confocal microscopy showed the punctate and perinuclear pattern of ND4FLAG immunofluorescence (*arrows*) surrounding RGC nuclei counterstained with DAPI appeared similar to the epifluorescence of a bona fide mitochondrial marker (mitochondria-specific fluorescent dye; *arrows*, **E**). (**F**) Merged panel shows RGCs with colocalization of ND4FLAG and the mitochondrial marker (*arrows*). (**G**) Low-power longitudinal cryostat sections revealed ND4FLAG immunofluorescence was confined to the RGC layer. Mitochondria-specific fluorescent dye accumulated in RGCs (**H**) and colocalized with ND4FLAG (**I**). (**J**) Higher power magnification revealed ND4FLAG immunofluorescence in RGCs, (**K**) mitochondria-specific fluorescent dye accumulation in RGC mitochondria, and (**L**) colocalization of mitochondria-specific fluorescent dye with ND4FLAG. Retinal nuclei were counterstained by DAPI (**D**–**L**). (**M**) Bar plot shows quantitative analysis of ND4FLAG- and GFP-positive cells. RGC, retinal ganglion cell layer; INL, inner nuclear layer.

Mitochondrial ultrastructure of RGCs revealed no evidence of hydropic degeneration or disruption of cristae (Fig. 5C). Internalized ND4FLAG-labeled immunogold was seen within RGC mitochondria (Fig. 5D). High magnification of mitochondria of axons of the optic nerve from an AAV-ND4FLAG–inoculated eye revealed normal cristae (Fig. 5E). Optic nerve mitochondria exhibited ND4FLAG immunogold within the organelle (Fig. 5F). Because the fixation and embedding media needed to preserve immunogold staining resulted in some loss of fine ultrastructure details, we identified mitochondria with a mitochondrial superoxide dismutase antibody (MnSOD) counterstained with 10 nm immunogold. The anti–FLAG antibody was

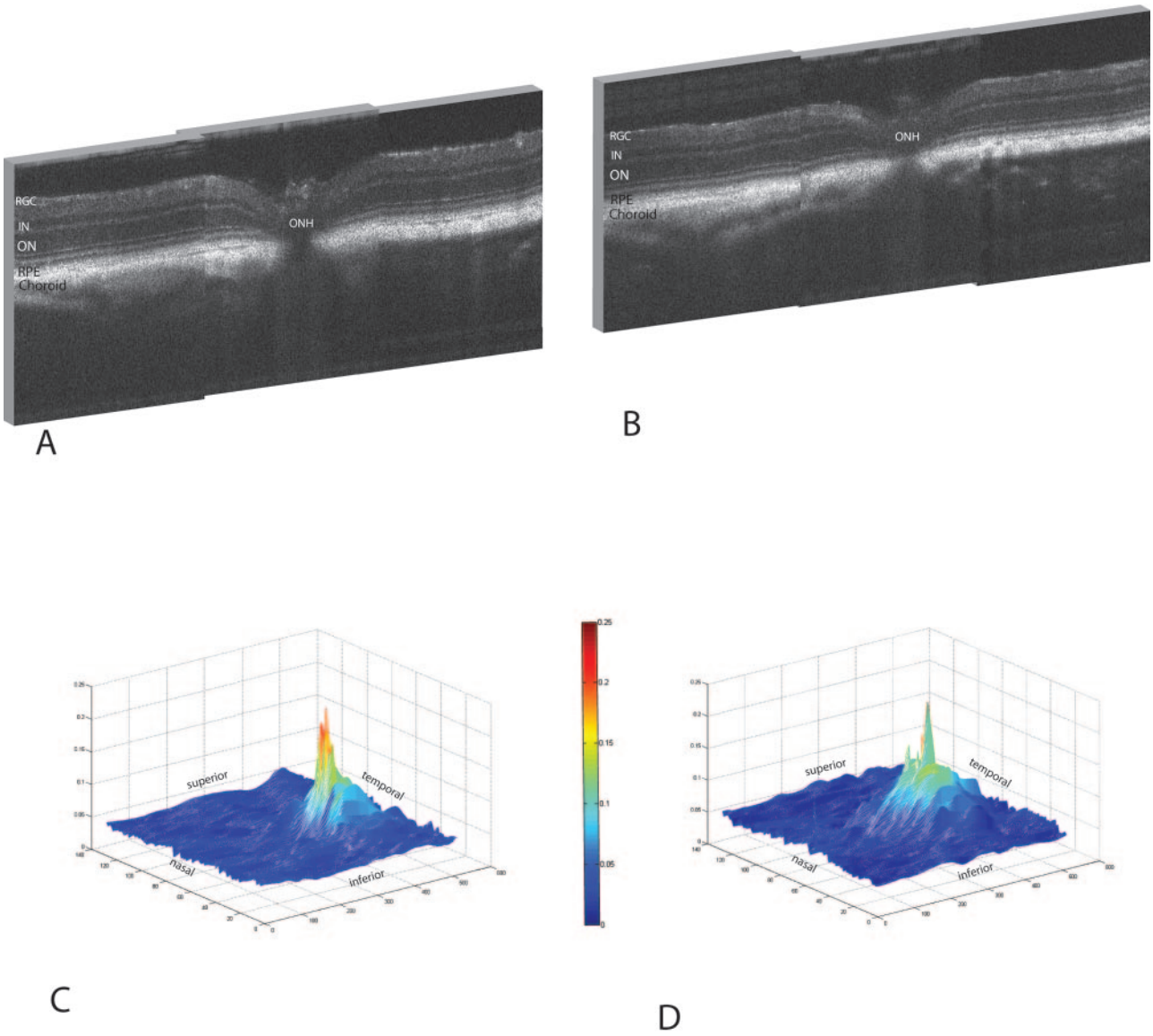

FIGURE 3. (**A**) Cross-sectional montaged images of the optic nerve head and peripapillary retina from the acquired 3D OCT data set of an AAV-ND4–inoculated mouse eye and the AAV-GFP–injected eye (**B**) show normal retinal anatomy. The OCT image is displayed in grayscale, with darker readings corresponding to lower backscattering (inner nuclear [IN] and outer nuclear [ON] layers) and brighter regions representing higher backscattering (RPE and choroid). RGC layers of experimental and control eyes were clearly recognizable. The optic nerve head of AAV-ND4 and control eyes showed no evidence of displacement of the peripapillary retina. With the use of algorithms for 3D segmentation, we measured the distance from the RGC layer to the inner boundary of the IN layer providing a geometric plot in three dimensions for the AAV-ND4 (**C**) and AAV-GFP (**D**) control eyes. Superior, inferior, nasal, and temporal quadrants are marked. The peak represents an artifact created by the measurement process and the vessels overlying the optic nerve head. Scale bar values are in millimeters. RPE, retinal pigment epithelium; ONH, optic nerve head.

counterstained with 6 nm immunogold. Figures 5G and 5H show colocalization of the smaller FLAG immunogold within the electron-dense organelles, which also contained the 10 nm MnSOD immunogold. These findings confirm translocation of the FLAG-tagged human ND4 into the mitochondria; they also confirm that the import of a cytoplasmically synthesized human mitochondrial protein does not alter the mitochondrial ultrastructure of the mouse optic nerve or retina.

Electrophysiology. Having demonstrated RGC expression of human ND4, we tested for physiological effects of this construct on the murine retina (six mice). We observed no differences in FERG signals between experimental and control eyes before AAV administration or 1 month after intraocular injections (data not presented). This indicated that the ND4 was not toxic to the retina. Focusing on the potential effect of human ND4 on murine RGCs was our next step. Before intraocular injections, mean PERG amplitudes were 17.8 ± 7.8 μV (mean ± SD) for the right eyes and 25.2 ± 12.2 μV for the left eyes. Mean PERG latency was 118.2 ± 17.5 ms for the right eyes and 98.8 ± 12.8 ms for the left eyes before AAV administration. PERG performed 1 month after intraocular injections showed no significant differences between their preinjection values. Figure 6A shows a normal PERG 1 month after AAV-ND4FLAG gene inoculation. The control eye of this animal injected with AAV-GFP is shown for comparison (Fig. 6B). One month after intravitreal injection, the mean PERG amplitude of AAV-NDFLAG–inoculated eyes was 10.9 ± 6.6 μV compared with a mean value of 13.2 ± 5.2 μV for AAV-GFP–inoculated eyes (Fig. 6C). Amplitude differences between experimental and control eyes were not statistically significant ($P = 0.48$).

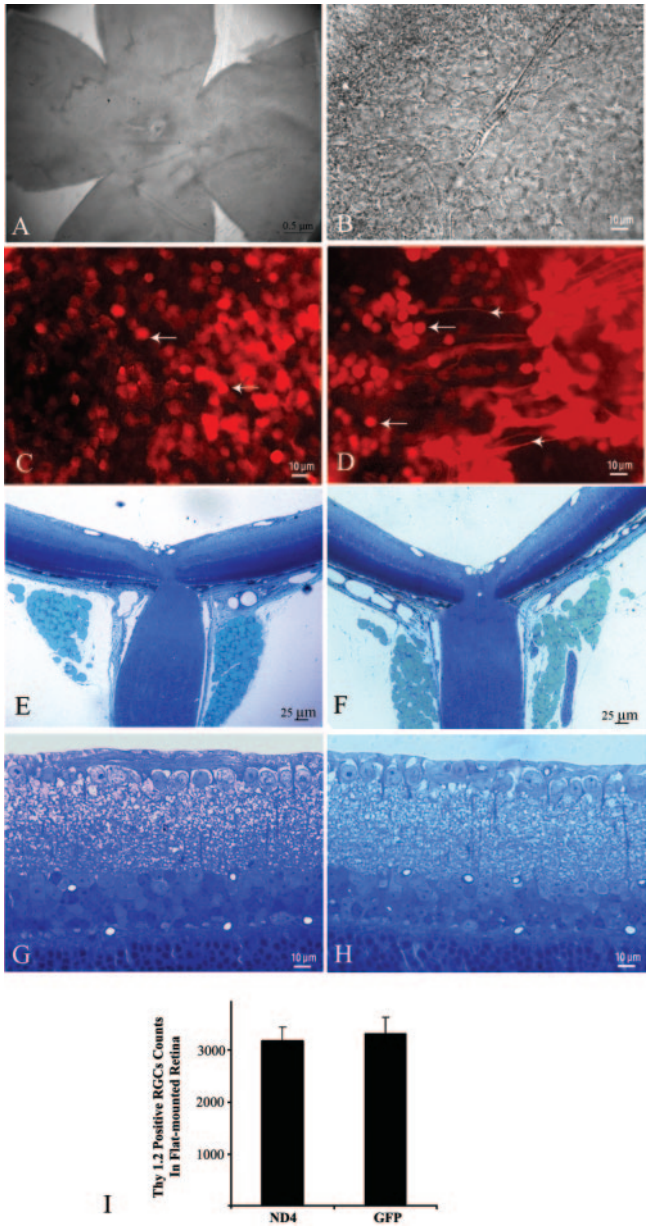

FIGURE 4. (**A**) Excised retina was laid out flat with the RGC layer facing upward. (**B**) Phase-contrast light micrograph focused on the RGC layer. AAV-ND4FLAG–inoculated (**C**) and AAV-GFP–inoculated (**D**) eyes show numerous labeled Thy1.2-positive RGCs (*arrows*). Toluidine blue sections of AAV-ND4FLAG–inoculated (**E**) or AAV-GFP–inoculated (**F**) eyes showed no evidence of swelling of the optic nerve head. RGCs of AAV-ND4FLAG–injected (**G**) or AAV-GFP–injected (**H**) eyes showed the absence of chromatolysis or loss. (**I**) Bar plot of Thy1.2-positive cells shows no significant differences in RGC counts between AAV-ND4FLAG– and AAV-GFP–infected eyes.

However, latency differences were statistically significant ($P = 0.015$). The mean PERG latency of ND4FLAG-inoculated eyes with a value of 103.7 ± 9.9 ms was shorter than a value of 130.3 ± 19.7 ms for GFP controls (Fig. 6D). Thus, the human ND4 did have a small, but measurable, nontoxic effect on murine RGC function.

ATP Synthesis. Last, we tested for potential alterations in the rate of ATP synthesis induced by incorporation of the human ND4 into a murine complex I (seven mice). The rate of ATP synthesis in eyes inoculated with human ND4 was 43.1 ± 35.6 nM ATP/mg protein (Fig. 7). The rate of ATP synthesis in control eyes inoculated with GFP was 56.6 ± 72.7 nM ATP/mg protein. These differences were not statistically significant ($P = 0.67$). Thus, human ND4 did not have an adverse impact on respiration of the mouse optic nerve.

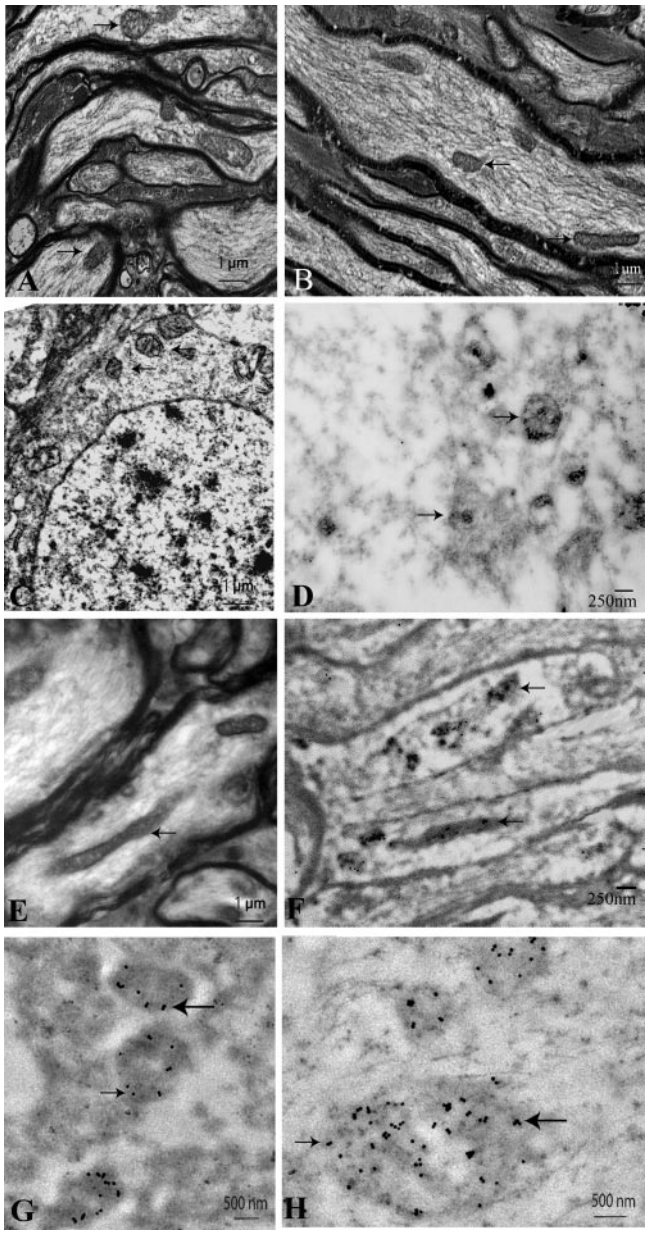

FIGURE 5. (**A**) Axons of the optic nerve obtained from an eye of a mouse that received no intraocular injection, and that of an AAV-ND4FLAG–inoculated eye (**B**) revealed normal structure of mitochondrial cristae (*arrow*) and axonal microtubules. (**C**) RGC of an AAV-ND4FLAG–injected eye exhibited a normal-appearing elliptical nucleus with pale chromatin and mitochondria with normal morphology of cristae (*arrow*). (**D**) Internalized NDFLAG-labeled immunogold (*arrows*) is seen within RGC mitochondria of a resin-embedded mouse retina. (**E**) High magnification of mitochondria (*arrow*) of axons of the optic nerve from an AAV-ND4FLAG–inoculated eye revealed normal cristae. (**F**) Optic nerve axonal mitochondria show ND4FLAG immunogold (*arrows*) within the organelles. (**G**, **H**) Double staining shows 6-nm anti–FLAG immunogold (*small arrow*) colocalizes with the larger 10-nm anti–MnSOD (*large arrow*) within mitochondria.

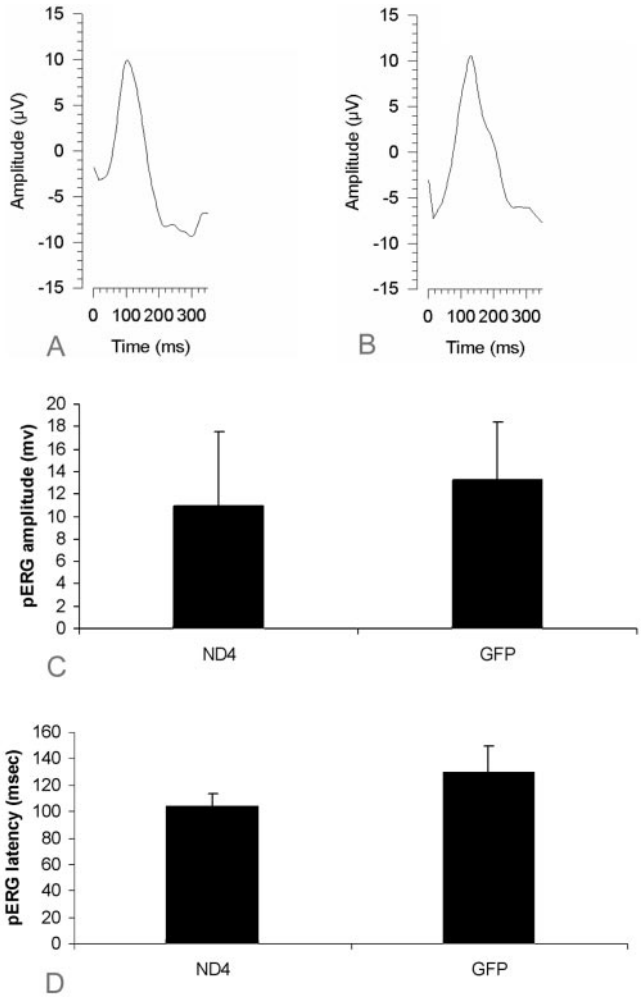

FIGURE 6. (**A**) Representative PERG of an ND4FLAG-inoculated eye and (**B**) PERG of the control eye of an animal injected with AAV-GFP. (**C**) Bar plot shows PERG amplitudes of ND4-inoculated eyes similar to those of GFP-inoculated eyes. (**D**) Bar plot of PERG latency shows a reduction in ND4-inoculated eyes compared with GFP controls.

DISCUSSION

Our understanding of human diseases caused by mutated mtDNA has recently advanced dramatically. This is a group of untreatable disorders affecting the eye, nervous system, and heart. Some mitochondrial diseases have been clinically characterized for more than a century, but they are now known to be a spectrum of molecularly defined diseases. We have chosen to start with one of the most severe, the G11778A mutation in mtDNA responsible for LHON, a disease renowned for causing blindness in later childhood and early adulthood. In previous work we have made major strides toward determining the pathogenesis and testing a potential treatment for LHON. First, we discovered that ND4 mutant cells undergo a severe reduction in ATP synthesis, even though mild reductions in complex I activity appear insufficient to induce disease.[8] No technology existed to introduce DNA directly into mitochondria, but we overcame this deficiency in oxidative phosphorylation by constructing a "nuclear version" of the mitochondrial gene, then targeted the cytoplasmically synthesized protein to the mitochondria by using a targeting sequence appended to the reading frame (allotopic expression). When delivered to cultured cells containing a mutant ND4, respiratory function was restored. Next, we created a bona fide animal model for LHON. With the use of site-directed mutagenesis of the nuclear version of ND4, we replaced the codon for arginine with that for histidine at position 340. Injection of this construct into the mouse visual system disrupted mitochondrial cytoarchitecture, elevated reactive oxygen species, induced swelling of the optic nerve head, and induced apoptosis, with a progressive demise of ganglion cells in the retina and their axons comprising the optic nerve.[13]

In contrast, we showed here that ocular expression of the wild-type human ND4 subunit appears safe. When injected into the mammalian visual system, an AAV containing the normal human ND4 subunit of complex I is expressed in ganglion cells of the retina and axons of the optic nerve, the very cells impacted by LHON.[17] Incorporation of a normal human ND4 into the murine complex I did not adversely impact ATP synthesis in the mouse optic nerve. Mitochondrial DNA is highly conserved. The human and mouse ND4 subunit of complex I have a nucleotide consensus of approximately two-thirds, whereas the amino acid consensus is much higher (82%). In both species an arginine is present in the ND4 subunit at amino acid 340. Some loss in ATP production might have been anticipated with a human version of ND4 incorporated into the mouse complex I. We did not find that here. In addition, the human ND4 did not reduce RGC counts in the mouse eye and did not significantly suppress the PERG amplitude, which is believed to be derived predominantly from RGCs. However, the human ND4 did have a measurable biological effect on mouse RGCs. It shortened the PERG latency. Amplitude and phase represent two distinct aspects of neural activity.[18–20] Response amplitude is related to the number and vitality of retinal neurons contributing to the recorded electrical signal. To a first approximation, the smaller the number of neurons activated by the visual stimulus the smaller the electrical signal; the sicker the neurons (and/or abnormal connectivity or gain relationships between neurons) the smaller the electrical signal. Clearly, human ND4 expression did not have an impact on RGC viability. Response latency is an additional index of vitality of activated neurons that may or may not be associated with amplitude reduction. Mechanisms of latency delay are understood less than they are of amplitude reduction. To a first approximation, the slower the electrical signal generated by activated neurons, the larger the latency delay. However, other possibilities cannot be excluded. One such possibility is that the time-to-peak of the major positive wave (used as index of PERG latency) is changed because the response *duration* is changed (the waveform becomes broader or nar-

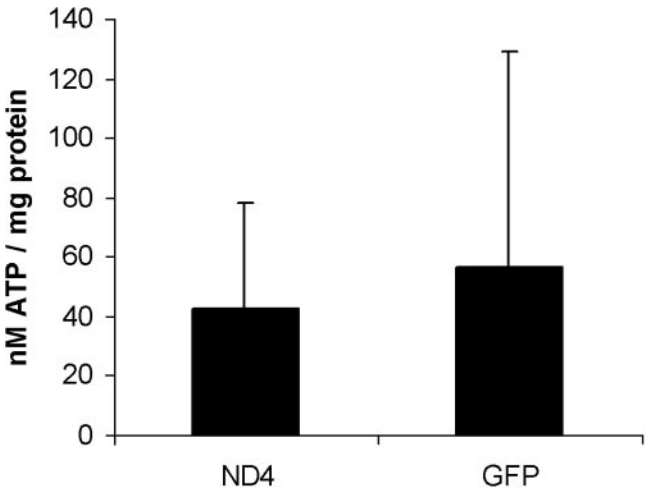

FIGURE 7. Bar plot shows optic nerve ATP synthesis in AAV-ND4– and AAV-GFP–inoculated eyes are comparable.

rower with likely changes in time to peak). Changes in response duration and associated changes in time to peak can be easily simulated by changing the settings of the low-pass and high-pass filters of the amplifiers. Changes in gain and bandpass characteristics of RGCs are possible in our experimental conditions, but we do not have evidence that either mechanism plays a role in the effects we have measured.

The wild-type version of the human ND4 subunit gene did not cause swelling of the optic nerve head or apoptosis of RGCs, findings that were previously seen at this juncture in mouse eyes inoculated with the mutant *ND4*.[13] In those studies, expression of the human mutant R340H ND4 exerted a dominant negative effect in the mouse, inducing loss of RGCs and optic neuropathy in the presence of normal murine ND4. Thus, the LHON animal model is unlike human LHON, which requires 100% mutated G11778A mtDNA for phenotypic expression of the visual loss.[13] Here histology and PERG of ganglion cells of wild-type ND4FLAG-infected retina appeared normal, suggesting that delivery of ND4 is feasible and safe in mammals and perhaps eventually in our patients with LHON. In vivo efficiency of allotopic expression of the human ND4 subunit complex in murine RGCs was 38%. Twenty-five percent lower efficiency of allotopic expression was reported by Ellouze et al.,[21] who used COX10 MTS to drive the import of human ND4, which was also optimized for mitochondrial expression with the 3′UTR of SOD2. In their study, which used electroporation for ocular gene delivery into RGCs of the rat, this slightly lower level of efficiency of allotopic expression of the normal human ND4 was sufficient for rescue of visual function and RGC loss induced by the mutant G11778A ND4. Unlike electroporation, which provides transient ocular gene expression, gene delivery with the AAV vector is stable for years.[22,23] Moreover, this vector and serotype (AAV2) have been used safely in a phase 1 human ocular gene therapy trial.[24] Newer AAV vectors such as the self-complementary AAV, which contains a double-stranded gene for delivery,[25–27] or other AAVs with mutations in the capsid proteins designed to reduce cellular AAV degradation[28,29] provide the promise of higher levels of allotopic ND4 efficiency than seen in our study.

Although experimental approaches have been used, such as importing genes from other species, changing the ratio of heteroplasmy with specific restriction endonucleases, selecting for respiratory function or regeneration (in muscle), none of these techniques is directly applicable to the treatment of LHON, which is caused by 100% mutated mtDNA.[30,31] Typically, patients with LHON have homoplasmic mutations, and they present with acute visual loss in one eye first and optic disc edema in both eyes. The fellow eye then loses vision in approximately 2 months. Rescue here would be the best possible scenario. It would suggest that treatment at the time of visual loss in the first eye, perhaps followed in several weeks by treatment to the fellow eye, may restore vision to the patient with LHON. Newman et al.[32] used topical brimonidine (Alphagan; Allergan, Irvine, CA) before optic nerve degeneration but were unable to avert visual and RGC loss in their patients with LHON. Perhaps oxidative injury and apoptosis are irreversible at this time.

Rescue of optic neuropathy in the rat[21] and our expression studies using the AAV vector suggest that allotopic *ND4* gene therapy may be effective in patients with LHON with the G11778A mtDNA mutation. That allotopic expression can rescue complex I deficiency was initially proven in a murine model of Parkinson disease. Rather than complementing the defective 8-kDa complex I subunit[33] with a human gene, the investigators used the AAV vector to deliver the single-subunit NADH dehydrogenase, NDI1, of yeast (*Saccharomyces cerevisiae*).[34] Despite the marked mismatch in the amino acid sequence and size of the yeast compared with the murine complex I, 50% rescue of complex I activity was seen in their mice.

We also proved here that the human ND4FLAG labeled by immunogold decorated the interior of mitochondria, thus confirming translocation of the FLAG-tagged ND4 into the organelle. This finding proves that the allotopic ND4 protein was not stuck in the mitochondrial import channels, as suggested by Oca-Cossio et al.[11] In addition, loss of mitochondrial membrane potential (accumulation of the mitochondria-specific fluorescent dye) and the cellular demise predicted by the studies of Oca-Cossio, et al.[11] were not seen in our mice, which exhibited normal ultrastructural RGC morphology and axonal mitochondria in human ND4-transfected eyes. Moreover, immunoprecipitation with the anti–FLAG antibody revealed the 52-kDa band of human ND4, thus indicating that it had integrated into the mouse complex I. The slightly higher molecular weight of uncleaved P1ND4FLAG seen in mitochondrial isolates was not evident,[13] suggesting that the nuclear encoded human ND4 complex I subunit imported into the mitochondria was processed by cleavage of the ATPc targeting sequence from the mature human ND4 fusion protein that was then incorporated into the mouse complex I we immunoprecipitated. Integration is an important step. Manfredi et al.[8] used allotopic P1ATP6FLAG to rescue ATP synthesis in a cell line with mutated T8993G mtDNA. This mutation is associated with maternally inherited Leigh syndrome and neurogenic ataxia retinitis pigmentosa. In later experiments by Bokori-Brown and Holt,[12] which used native blue gel two-dimensional electrophoresis, the allotopically expressed ATP6 subunit, including the Manfredi construct, did not appear to integrate into the ATP synthase.

Despite the apparent controversies in vitro, we believe that the cumulative in vivo data to date provide convincing evidence that allotopic gene delivery is safe and that it may eventually prove useful in the treatment of patients with LHON with mutated mtDNA; such patients are now being enrolled in our clinical study. Still, long-term evaluation of *ND4* gene expression and safety studies in nonhuman primates, which we are planning, are needed before a phase 1 clinical trial. Success here may have implications well beyond these initially targeted patients and for organ systems other than the eye.

Acknowledgments

The authors thank Liang Sun for technical expertise in performing the RT-PCR and immunoprecipitation experiments and Mabel Wilson for editing the manuscript.

References

1. Wallace DC, Singh G, Lott MT, et al. Mitochondrial DNA mutation associated with Leber hereditary optic neuropathy. *Science.* 1988; 242:1427–1430.
2. Esposito LA, Melov S, Panov A, et al. Mitochondrial disease in mouse results in increased oxidative stress. *Proc Natl Acad Sci U S A.* 1999;96:4820–4825.
3. Carelli V, Ghelli A, Bucchi L, et al. Biochemical features of mtDNA 14484 (ND6/M64V) point mutation associated with Leber's hereditary optic neuropathy. *Ann Neurol.* 1999;45:320–328.
4. Glick B, Schatz G. Import of proteins into mitochondria. *Annu Rev Genet.* 1991;25:21–44.
5. Neupert W. Protein import into mitochondria. *Annu Rev Biochem.* 1997;66:863–917.
6. Nagley P, Farrell LB, Gearing DP, et al. Assembly of functional proton-translocating ATPase complex in yeast mitochondria with cytoplasmically synthesized subunit 8, a polypeptide normally encoded within the organelle. *Proc Natl Acad Sci U S A.* 1988;85: 2091–2095.

7. Owen R IV, Lewin AP, Peel A, et al. Recombinant adeno-associated virus vector-based gene transfer for defects in oxidative metabolism. *Hum Gene Ther.* 2000;11:2067–2078.
8. Guy J, Qi X, Pallotti F, et al. Rescue of a mitochondrial deficiency causing Leber hereditary optic neuropathy. *Ann Neurol.* 2002;52:534–542.
9. Manfredi G, Fu J, Ojaimi J, et al. Rescue of a deficiency in ATP synthesis by transfer of MTATP6, a mitochondrial DNA-encoded gene, to the nucleus. *Nat Genet.* 2002;30:394–399.
10. Claros MG, Perea J, Shu Y, et al. Limitations to in vivo import of hydrophobic proteins into yeast mitochondria: the case of a cytoplasmically synthesized apocytochrome b. *Eur J Biochem.* 1995;228:762–771.
11. Oca-Cossio J, Kenyon L, Hao H, et al. Limitations of allotopic expression of mitochondrial genes in mammalian cells. *Genetics.* 2003;165:707–720.
12. Bokori-Brown M, Holt IJ. Expression of algal nuclear ATP synthase subunit 6 in human cells results in protein targeting to mitochondria but no assembly into ATP synthase. *Rejuvenation Res.* 2006;9:455–469.
13. Qi X, Sun L, Lewin AS, et al. The mutant human ND4 subunit of complex I induces optic neuropathy in the mouse. *Invest Ophthalmol Vis Sci.* 2007;48:1–10.
14. Hauswirth WW, Lewin AS, Zolotukhin S, et al. Production and purification of recombinant adeno-associated virus. *Methods Enzymol.* 2000;316:743–761.
15. Ruggeri M, Wehbe H, Jiao S, et al. In vivo three-dimensional high-resolution imaging of rodent retina with spectral-domain optical coherence tomography. *Invest Ophthalmol Vis Sci.* 2007;48:1808–1814.
16. Porciatti V. The mouse pattern electroretinogram. *Doc Ophthalmol.* 2007;115:145–153.
17. Carelli V, Ross-Cisneros FN, Sadun AA. Optic nerve degeneration and mitochondrial dysfunction: genetic and acquired optic neuropathies. *Neurochem Int.* 2002;40:573–584.
18. Porciatti V, Ventura LM. Adaptive changes of inner retina function in response to sustained pattern stimulation. *Vision Res.* 2009;49:505–513.
19. Ventura LM, Sorokac N, De Los SR, et al. The relationship between retinal ganglion cell function and retinal nerve fiber thickness in early glaucoma. *Invest Ophthalmol Vis Sci.* 2006;47:3904–3911.
20. Ventura LM, Porciatti V. Pattern electroretinogram in glaucoma. *Curr Opin Ophthalmol.* 2006;17:196–202.
21. Ellouze S, Augustin S, Bouaita A, et al. Optimized allotopic expression of the human mitochondrial ND4 prevents blindness in a rat model of mitochondrial dysfunction. *Am J Hum Genet.* 2008;83:373–387.
22. Dudus L, Anand V, Acland GM, et al. Persistent transgene product in retina, optic nerve and brain after intraocular injection of rAAV. *Vision Res.* 1999;39:2545–2553.
23. Guy J, Qi X, Muzyczka N, et al. Reporter expression persists 1 year after adeno-associated virus-mediated gene transfer to the optic nerve. *Arch Ophthalmol.* 1999;117:929–937.
24. Hauswirth W, Aleman TS, Kaushal S, et al. Phase I trial of Leber congenital amaurosis due to RPE65 mutations by ocular subretinal injection of adeno-associated virus gene vector: short-term results. *Hum Gene Ther.* 2008;19:979–990.
25. McCarty DM. Self-complementary AAV vectors; advances and applications. *Mol Ther.* 2008;16:1648–1656.
26. McCarty DM, Monahan PE, Samulski RJ. Self-complementary recombinant adeno-associated virus (scAAV) vectors promote efficient transduction independently of DNA synthesis. *Gene Ther.* 2001;8:1248–1254.
27. McCarty DM, Fu H, Monahan PE, et al. Adeno-associated virus terminal repeat (TR) mutant generates self-complementary vectors to overcome the rate-limiting step to transduction in vivo. *Gene Ther.* 2003;10:2112–2118.
28. Zhong L, Li B, Jayandharan G, et al. Tyrosine-phosphorylation of AAV2 vectors and its consequences on viral intracellular trafficking and transgene expression. *Virology.* 2008;381:194–202.
29. Zhong L, Li B, Mah CS, et al. Next generation of adeno-associated virus 2 vectors: point mutations in tyrosines lead to high-efficiency transduction at lower doses. *Proc Natl Acad Sci U S A.* 2008;105:7827–7832.
30. DiMauro S, Hirano M, Schon EA. Approaches to the treatment of mitochondrial diseases. *Muscle Nerve.* 2006;34:265–283.
31. Bayona-Bafaluy MP, Blits B, Battersby BJ, et al. Rapid directional shift of mitochondrial DNA heteroplasmy in animal tissues by a mitochondrially targeted restriction endonuclease. *Proc Natl Acad Sci U S A.* 2005;102:14392–14397.
32. Newman NJ, Biousse V, David R, et al. Prophylaxis for second eye involvement in Leber hereditary optic neuropathy: an open-labeled, nonrandomized multicenter trial of topical brimonidine purite. *Am J Ophthalmol.* 2005;140:407–415.
33. Keeney PM, Xie J, Capaldi RA, et al. Parkinson's disease brain mitochondrial complex I has oxidatively damaged subunits and is functionally impaired and misassembled. *J Neurosci.* 2006;26:5256–5264.
34. Seo BB, Nakamaru-Ogiso E, Flotte TR, et al. In vivo complementation of complex I by the yeast Ndi1 enzyme: possible application for treatment of Parkinson disease. *J Biol Chem.* 2006;281:14250–14255.